



**HAL**  
open science

## Resilience of Snowball Earth to Stochastic Events

Guillaume Chaverot, Andrea Zorzi, Xuesong Ding, Jonathan Itcovitz, Bowen Fan, Siddharth Bhatnagar, Aoshuang Ji, Robert J. Graham, Tushar Mittal

► **To cite this version:**

Guillaume Chaverot, Andrea Zorzi, Xuesong Ding, Jonathan Itcovitz, Bowen Fan, et al.. Resilience of Snowball Earth to Stochastic Events. *Geophysical Research Letters*, 2024, 51, 10.1029/2024GL109512 . insu-04836842

**HAL Id: insu-04836842**

**<https://insu.hal.science/insu-04836842v1>**

Submitted on 14 Dec 2024

**HAL** is a multi-disciplinary open access archive for the deposit and dissemination of scientific research documents, whether they are published or not. The documents may come from teaching and research institutions in France or abroad, or from public or private research centers.

L'archive ouverte pluridisciplinaire **HAL**, est destinée au dépôt et à la diffusion de documents scientifiques de niveau recherche, publiés ou non, émanant des établissements d'enseignement et de recherche français ou étrangers, des laboratoires publics ou privés.



Distributed under a Creative Commons Attribution 4.0 International License

# Geophysical Research Letters<sup>®</sup>



## RESEARCH LETTER

10.1029/2024GL109512

## Resilience of Snowball Earth to Stochastic Events

Guillaume Chaverot<sup>1,2,3</sup> , Andrea Zorzi<sup>4</sup> , Xuesong Ding<sup>5,6</sup> , Jonathan Itcovitz<sup>7,8</sup> , Bowen Fan<sup>9</sup> , Siddharth Bhatnagar<sup>1,3,10</sup> , Aoshuang Ji<sup>11</sup> , Robert J. Graham<sup>9</sup> , and Tushar Mittal<sup>11</sup>

### Key Points:

- We use an Energy Balance Model (EBM) to simulate the response of Snowball climate after stochastic events
- Impact simulations and estimates of ash dispersion are used to inform initial conditions
- Earth's Snowball states seem resilient to termination by stochastic events within our modeling framework

<sup>1</sup>Observatoire Astronomique de l'Université de Genève, Versoix, Switzerland, <sup>2</sup>Université Grenoble Alpes, CNRS, IPAG, Grenoble, France, <sup>3</sup>Life in the Universe Center, Geneva, Switzerland, <sup>4</sup>Department of Earth and Planetary Sciences, Stanford University, Stanford, CA, USA, <sup>5</sup>Department of Earth, Planetary, and Space Sciences, University of California, Los Angeles, CA, USA, <sup>6</sup>Now at Bureau of Economic Geology, The University of Texas at Austin, Austin, TX, USA, <sup>7</sup>Institute of Astronomy, University of Cambridge, Cambridge, UK, <sup>8</sup>Department of Civil and Environmental Engineering, Imperial College London, London, UK, <sup>9</sup>Department of the Geophysical Sciences, University of Chicago, Chicago, IL, USA, <sup>10</sup>Group of Applied Physics and Institute for Environmental Sciences, University of Geneva, Geneva, Switzerland, <sup>11</sup>Department of Geosciences, Pennsylvania State University, University Park, PA, USA

### Supporting Information:

Supporting Information may be found in the online version of this article.

### Correspondence to:

G. Chaverot,  
guillaume.chaverot@univ-grenoble-alpes.fr

### Citation:

Chaverot, G., Zorzi, A., Ding, X., Itcovitz, J., Fan, B., Bhatnagar, S., et al. (2024). Resilience of snowball Earth to stochastic events. *Geophysical Research Letters*, 51, e2024GL109512. <https://doi.org/10.1029/2024GL109512>

Received 27 MAR 2024

Accepted 9 JUL 2024

### Author Contributions:

**Conceptualization:** Guillaume Chaverot, Bowen Fan

**Data curation:** Guillaume Chaverot, Andrea Zorzi, Jonathan Itcovitz

**Investigation:** Guillaume Chaverot

**Methodology:** Guillaume Chaverot, Andrea Zorzi, Xuesong Ding, Jonathan Itcovitz, Bowen Fan, Siddharth Bhatnagar, Aoshuang Ji, Tushar Mittal

### Project administration:

Guillaume Chaverot, Andrea Zorzi

### Writing – original draft:

Guillaume Chaverot, Andrea Zorzi

### Writing – review & editing:

Guillaume Chaverot, Andrea Zorzi, Xuesong Ding, Jonathan Itcovitz, Bowen Fan, Siddharth Bhatnagar, Robert J. Graham, Tushar Mittal

© 2024. The Author(s).

This is an open access article under the terms of the [Creative Commons Attribution License](https://creativecommons.org/licenses/by/4.0/), which permits use, distribution and reproduction in any medium, provided the original work is properly cited.

**Abstract** Earth went through at least two periods of global glaciation (i.e., “Snowball Earth” states) during the Neoproterozoic, the shortest of which (the Marinoan) may not have lasted sufficiently long for its termination to be explained by the gradual volcanic build-up of greenhouse gases in the atmosphere. Large asteroid impacts and supervolcanic eruptions have been suggested as stochastic geological events that could cause a sudden end to global glaciation via a runaway melting process. Here, we employ an energy balance climate model to simulate the evolution of Snowball Earth's surface temperature after such events. We find that even a large impactor (diameters of  $d \sim 100$  km) and the supervolcanic Toba eruption (74 Kyr ago), are insufficient to terminate a Snowball state unless background CO<sub>2</sub> has already been driven to high levels by long-term outgassing. We suggest, according to our modeling framework, that Earth's Snowball states would have been resilient to termination by stochastic events.

**Plain Language Summary** The terminations of Earth's longest periods of global glaciation are commonly understood to have occurred due to the gradual build-up of greenhouse gases in the atmosphere from volcanism. However, the sudden ends of Earth's shorter global glaciation periods likely cannot be explained by the same mechanisms. Large asteroid impacts and supervolcanic eruptions have been suggested as geophysical phenomena that could cause abrupt ends to global glaciation periods. Here, we model the evolution of the planet's surface temperature in the aftermath of such events. Impacts and eruptions open up gaps in the global ice sheet, and also partially cover the ice in far-spreading dust and ash, both of which increase the amount of solar radiation that is absorbed by the planet comparing to the highly reflective surface of ice and snow. Greater absorption of radiation leads to higher surface temperatures, which increases ice melting, and generates a feedback loop that can melt the entire planet surface. However, we find that the scales of impact or eruption required to produce global melting are too great to have likely occurred at the times of Earth's global glaciations. Other mechanisms must, therefore, be explored to explain Earth's short glaciation periods.

## 1. Introduction

The Snowball Earth hypothesis (Hoffman et al., 1998, 2017; Kirschvink, 1992) proposes global surface coverage of Earth in a thick ice layer. In contrast, the most recent glacial episode, the Last Glacial Period, witnessed only partial ice coverage extending down from the poles but not reaching equatorial regions (e.g., Batchelor et al., 2019). Snowball events have occurred on at least two occasions during the Neoproterozoic era (1,000–538.8 Ma). In particular, there is good evidence for a snowball event during the Cryogenian period (720–635 Ma), with other potential Snowball states also being suggested (e.g., Chumakov, 2009). Evidence for Snowball Earth's existence comes in many forms, including paleomagnetic data in Australia (Hambrey & Harland, 1981; Harland, 1964), Australian cap carbonates (Kennedy, 1996), and extreme carbon isotope excursions in Norway and Greenland (Knoll et al., 1986). Geologic measurements have been complemented by modeling efforts (e.g., Caldeira & Kasting, 1992) to understand both the origins and demise of the Snowball state.

Under Earth's current insolation, a Snowball state is one of three possible stable climate regimes for Earth, alongside a temperate state and a hot steam atmosphere state (Shields et al., 2014; Turbet et al., 2021). However,

as shown in Brunetti et al. (2019), the number and nature of these stable climate regimes can vary depending on feedbacks considered within the model. The Snowball state is stable against moderate variations in insolation through the high albedo of ice, which acts to prevent increases in global temperature (Hoffman et al., 2017; Shields et al., 2014). This creates a bi-stability between the temperate Earth and Snowball Earth through the difference of albedo between ice and liquid water (Ghil, 1994). It is, therefore, impossible to deglaciate Snowball Earth under such conditions without other climate forcings. One such forcing that is commonly invoked is the build-up of atmospheric CO<sub>2</sub> (Menou, 2015; Walker et al., 1981). Magmatic volatile emissions from volcanism, coupled with the absence of CO<sub>2</sub> sinks of Earth's temperate-state carbon cycle (e.g., silicate weathering being prevented by the covering of ice) leads to a strong greenhouse effect that warms the planet, triggering the Snowball termination (Caldeira & Kasting, 1992; Kirschvink, 1992). However, the time required to accumulate sufficient CO<sub>2</sub> to trigger melting (4–30 Myr, Hoffman et al., 1998) is too long to account for the short Marinoan glaciation (Rooney et al., 2015). Suggested alternatives include impact events (Kring, 2003) and massive volcanic eruptions (Lan et al., 2022), which we hereafter refer to as stochastic events due to the nature of their occurrences. However, quantitative estimates of climate after stochastic events remain relatively unexplored.

Impacts of large asteroids can generate global climate effects (e.g., Artemieva et al., 2017; Brugger et al., 2017; Pierazzo et al., 1998; Turbet et al., 2020). Simulations of such impacts have estimated the masses of water vapor injected into the atmosphere by these events, but the climatic implications have not been investigated (Koeberl & Ivanov, 2019) or have been inconclusive due to uncertainties on the radiative effect of water vapor (Erickson et al., 2020). Nonetheless, the temporal coincidence between the youngest Paleoproterozoic glacial deposits and the Yarrabubba event has sparked interest in the role of impacts in climate evolution (Erickson et al., 2020). Further, given their large kinetic energy, impacts can melt the ice table covering the planet surface and vapourize rocks from the underlying crust. Therefore, among other effects, impacts can (a) increase the planet's surface temperature by hundreds of degrees for large distances from the impact site, and (b) deposit ejecta material onto the icy surface far from the impact site, affecting the planet's surface albedo.

Supervolcanic eruptions are also suggested candidates to escape the Snowball Earth state. Such events are defined by either their magnitude ( $M \geq 8$ , proportional to the erupted mass) or their ejecta volume (1,000 km<sup>3</sup>, de Silva & Self, 2022), and are thousands of times larger than typical volcanic eruptions (e.g., Hansen et al., 1978). The largest known super-eruption is Toba ( $M = 9.1$ ), which is recorded in the 74,000-year-old Youngest Toba Tuff (YTT, Rose & Chesner, 1990). The ash ejected by the event covered ~40 million km<sup>2</sup> of Earth's surface at a depth greater than 5 mm (Costa et al., 2014). Toba-like super-eruptions are expected to happen 1–2 times per million years (Cisneros de León et al., 2022; Mason et al., 2004). Supervolcanic eruptions have significant global climate effects (e.g., Hansen et al., 1978). Large volumes of volcanic gases are injected into the atmosphere, such as (a) CO<sub>2</sub>, which acts as a classical greenhouse gas, (b) SO<sub>2</sub>, which acts as a solar-reflecting coolant, and (c) H<sub>2</sub>O, which can act as a greenhouse gas, but can also form radiative-active clouds. Further, eruptions deposit ash and dust on the icy surface, reducing the albedo in comparison to clean ice and hence increasing the amount of sunlight absorbed by the planet's surface. Although often cited as a possible cause of the onset of global glaciation (Macdonald & Wordsworth, 2017), there is no detailed exploration of the viability of this scenario.

In this study, we quantify the heating effects of stochastic events on a globally glaciated Earth, testing the potential of such events to generate a runaway melting process that would lead to the termination of the Snowball state. Through impact simulations and ash-/ejecta-dispersal modeling (Sections 2.2 and 2.3), we quantify the changes in albedo and surface temperature produced by such events. Using a 1-D Energy Balance Model (EBM; Section 2.1), we then analyze the radiative perturbation caused by such temperature and albedo changes, following the evolution of the post-event surface temperature profile and ice coverage. By varying the scale of our stochastic events (e.g., impactor size, magnitude of supervolcanic eruption), we assess the capabilities of such events to trigger global deglaciation (Section 3). We discuss the likelihood of occurrence of our event scales during the Neoproterozoic, and thus the likelihood of deglaciation by stochastic events, in Section 4.

## 2. Method

### 2.1. Climate Modeling

Budyko (1969) and Sellers (1969)'s independent seminal works on the Earth's climate established the usefulness and robustness of 1-D EBMs. In a latitudinal EBM, the prognostic surface temperature is zonally averaged, thus leaving only the meridional dimension. This gives a remarkably good first-order estimate to solving the climate of

a rocky planet (Dressing et al., 2010; North & Coakley, 1979; Spiegel et al., 2008). The 1D-nature of the planet is further exemplified by parameterizing the meridional atmospheric heat transport as temperature-driven diffusion. Because bi-stability between the temperate Earth and Snowball Earth is a radiative balance process that exists through the difference of albedo between ice and liquid water (Ghil, 1994), we use an EBM focused on radiative balance (Dressing et al., 2010; Spiegel et al., 2008; Williams et al., 1998) to model the evolution of snowball deglaciation. The corresponding temperate and snowball temperature profiles are shown in Figure S2 in Supporting Information S1. As 1-D EBMs are not longitudinally defined, we developed a method to account for spatially-located events, correcting input calculations from impact simulations and estimations of ash-dispersion from eruptions (see Text S4 in Supporting Information S1).

For our simulations, we assume a planet following a circular orbit at 1 AU around a Sun-like star, with a modern Earth solar constant. We fix the planetary obliquity to  $0^\circ$  and also assume zero eccentricity. Land and oceans are uniformly distributed across the planet such that each latitude cell consists of a 70:30 modern Earth ocean-to-land ratio. Heat capacity and albedo parameterizations between ice and liquid water are smooth transition functions taken from Williams and Kasting (1997) and Spiegel et al. (2008) (see Text S4 in Supporting Information S1). To constrain our study within a simple framework, we neglect the effects of aerosols and ice-melting latent heat: potential caveats from our assumptions are discussed in Section 4. However, the neglected processes (e.g., dust enrichment of the stratosphere due to impacts,  $\text{SO}_2$  production of volcanism) tend to cool the atmosphere, making deglaciation more difficult to achieve. Even in these conditions, a significant warming of the planet is hardly reachable as shown in Section 3. Nonetheless, we account for variable relative humidity, cloud forcing (Abbot, 2014) and the potential addition of  $\text{CO}_2$  released by volcanic eruptions. We also evaluate the influence of the location of stochastic events by modeling eruptions and impacts at the equator and at  $40^\circ\text{N}$ . The effect of impacts is modeled by modifying the initial temperature distribution as per hydrocode simulations (see Section 2.2). Eruptions do not modify the temperature distribution, but affect the surface albedo due to ash-dispersion.

## 2.2. Impact Simulations

We use the shock physics code iSALE (Collins et al., 2016) to model asteroidal impacts on a Snowball Earth state and produce 1-D thermal profiles for the surface of the planet in the aftermath of the impact. We additionally analyze the spread of the impact ejecta curtain in order to estimate the reduction in surface albedo associated with covering the ice with ejecta material.

We initialize simulations based on estimates of Snowball Earth's surface state (Hoffman et al., 1998). A 5 km thick global ice sheet thus sits at the surface of the target planet, with a rocky crust, mantle, and iron core sitting below. An average surface temperature of 227 K is prescribed for the pre-impact temperature profile, matching the steady-state temperature found by the EBM in the absence of a stochastic climate forcing event. Impactors consist entirely of dunite, matching closely the thermodynamic behaviors of the chondritic material that are expected from such objects (Benz et al., 1989). We run simulations for impactors with diameters between 40 and 100 km to assess the effects of impact scale. The impact velocity is constant for all impacts at  $1.5\times$  mutual escape velocity ( $v_{\text{esc}}$ ), representing the most likely impact velocity (Chyba, 1991; Le Feuvre & Wicczorek, 2011), and we consider only head-on collisions, which is an approximation accounting for the small mass of the impactors relative to the Earth (more informations about the impact setup are provided in Text S2 in Supporting Information S1).

Simulations are run until the motion in the mantle region excavated by the impact settles out (i.e., the mantle has rebounded and subsequent oscillatory motions have terminated). A 1-D surface temperature profile is then extracted, and used as the initial perturbation of the EBM. Because we use a 1-D latitudinal EBM, the initial temperature at the impact site results from the average of the high-temperature impact site longitudes and the low-temperature unperturbed longitudes (see Text S4 in Supporting Information S1 for more details). As a result, the initial temperature in the EBM (zonal mean temperature, 200–350 K) is lower than the temperature at the impact site (local temperature,  $>1,000$  K). We find that this approach slightly facilitates deglaciation by marginally overestimating the surface albedo ( $<1\%$ ).

An albedo profile is similarly determined, accounting for the exposure of crustal material after melting of the ice layer and the deposition of material from the impact ejecta curtain on top of the ice table outside of the impact crater. We assume that ejecta reaches distances up to  $5\times$  the crater radius (e.g., Richardson et al., 2005), corresponding to

distances of 2,250, 3,850, 3,900, and 5,000 km from the impact site for the 40, 60, 80, and 100 km impactors, respectively. The albedo for ejecta-covered areas is set to 0.2, similar to that of cryoconite (Hotaling et al., 2021). A step-like transition is then assumed between dark ejecta and ice albedo (0.7). Finally, we re-scale the temperature increase with the surface area that is affected by the impact and the size of latitudinal band, assuming the impact energy is conserved during the zonal transport. The temperature rise is submitted as the input to the EBM.

### 2.3. Supervolcanic Eruptions

We implement the formalism of Pyle (1989) to model the variation of volcanic ash thickness ( $d$ ) with distance from the eruption center. The exponential relationship between  $d$  and the isopach area  $A_{\text{iso}}$  is given by:

$$d = d_0 e^{-kA_{\text{iso}}^{1/2}} \quad (1)$$

where  $d_0$  is the ash maximum thickness (units of m) and  $k$  is the rate of ash thinning with isopach area, also in m (Pyle, 1989). We find  $k$  using ( $d, A_{\text{iso}}$ ) values of volcanic ash fall from Toba, reconstructed through several tens of thickness measurements of the YTT tephra deposit (Costa et al., 2014) and digitized with QGIS (QGIS Development Team, 2024).

The ash deposition region is divided into fully- ( $d > 0.014$  mm) and partially-covered ( $0.002 < d < 0.014$  mm), the latter known as dusty ice (Le Hir et al., 2010). Assuming an elliptical geometry for ash-dispersal, the ash deposition area is converted in latitude and longitude. For Toba, the fully-covered area extends for  $\pm 43^\circ$  in latitude and  $\pm 86^\circ$  in longitude; the dusty ice area spans a wider range between  $\pm 50^\circ$  in latitude and  $\pm 100^\circ$  in longitude. At visible wavelengths, coarse dust has an albedo of 0.18 (Warren, 1982). Thus, assuming a clean ice albedo of 0.7, we assign the dusty ice albedo as changing linearly between clean ice and dust (Figure S3 in Supporting Information S1). Such values are consistent with measurements of bare ice mean albedo (Warren et al., 2002). Fine dust correspond to higher albedo values, thus making deglaciation harder (Flanner et al., 2021).

## 3. Results

The EBM is able to provide the temporal evolution of surface temperature for up to several years after the moment of climate forcing. We find, however, that temperatures tend to converge within around 2 years (e.g., Figure 1). Geospatial variation in temperature, due to the regional nature of the stochastic events, can be well represented by recording global temperature minima, maxima, and mean averages (Figure 1).

We first analyzed the effects of a Toba-like eruption (Figures 1a–1d) for a cloud-free atmosphere similar to the present-day Earth atmosphere, with variable water vapor, 1 bar of nitrogen and 400 ppm of  $\text{CO}_2$ , and with the eruption happening at the equator (Figure 1a). Additional simulations then included cloud radiative effects ( $14 \text{ W m}^{-2}$ , Abbot, 2014) and increased atmospheric  $\text{CO}_2$  at 800 ppm (Figure 1b) in order to test the robustness of the result to initial atmospheric conditions, and to account for greenhouse gases released by the eruption. Finally, we repeated these set simulations with the climate forcing occurring at  $40^\circ\text{N}$  (Figure 1c). In none of these simulations does a Toba-like eruption change surface temperatures sufficiently to escape the Snowball state. In the best-case scenario for deglaciation (i.e., accounting for the cloud-warming effect and with 800 ppm of  $\text{CO}_2$ ), the maximum equatorial temperature is only 255 K after relaxation from forcing. Other effects were further tested, but were found to contribute minorly to results within realistic bounds, including: the addition of humidity due to volcanic moisture, weaker atmospheric circulation, different ice albedo, and greater effective stellar insolation (see Text S5 and Figure S1 in Supporting Information S1).

In the case of our impactors, the largest ( $d = 100$  km) generates a transient water belt (note this may not be a true water belt but rather a function of the EBM's spatial structure), with maximum extents of  $4.5^\circ\text{N}$  and  $4.5^\circ\text{S}$ , and lasting for around 2 months (Figure 1h). During this time, the surface temperature of the planet decreases due to thermal emission. Once the freezing point is reached, the change of albedo induces a rapid runaway re-glaciation of the transient water belt. We thus find that even the 100 km impactor cannot melt a surface large enough to break the ice albedo feedback, which prevents the Snowball Earth deglaciation. The lower resultant temperatures and reduced geospatial domain of our smaller impactors ( $d = 40\text{--}80$  km) results in no production of a water belt and indeed limited melting of the planet's surface (Figures 1e–1g), with the same result of no deglaciation. Impactors larger than 100 km will melt more ice and will generate greater temperature perturbations. However, such impacts

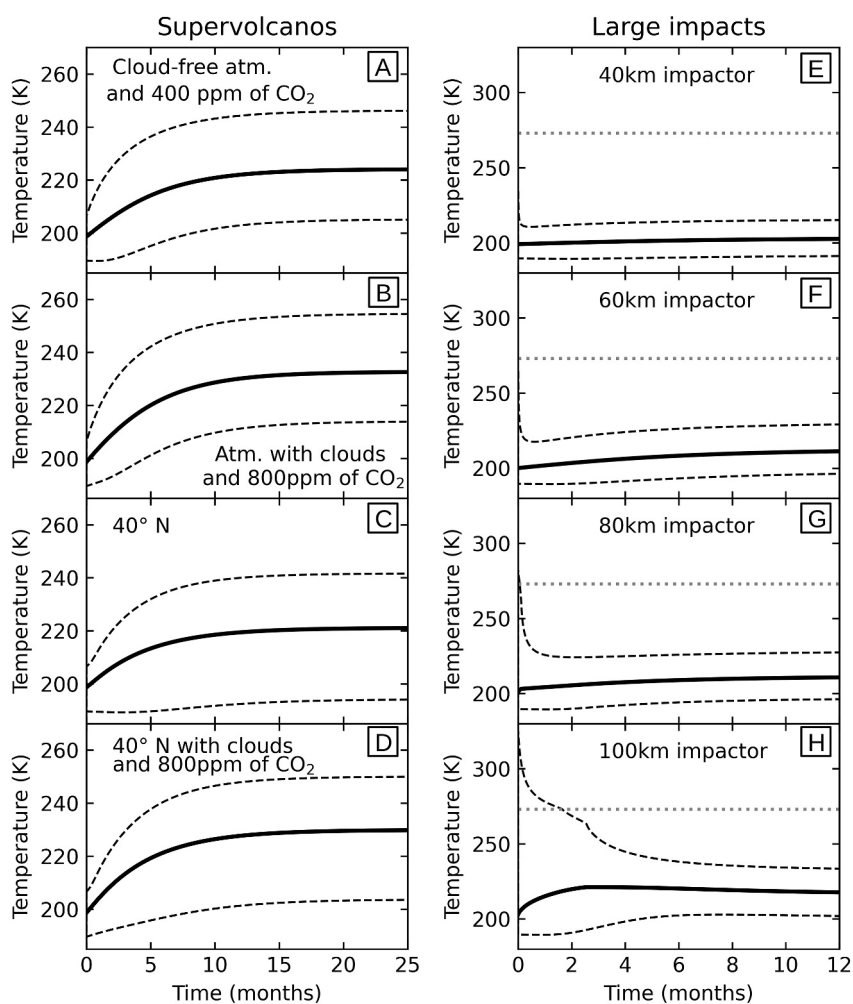


**Figure 1.** Temporal evolution of surface temperature after a Toba-like eruption (panel a–d) and impacts of varying size (panel e–h). For the eruptions, each panel corresponds to a different set of initial conditions, highlighting the differences that such effects produce under the same climate forcing event. For the impacts, all panels show the same cloud-free atmosphere with 400 ppm CO<sub>2</sub> of (a). The global-mean temperature (solid lines), minimum and maximum temperatures (dashed lines), and the melting temperature of the surface ice (dotted lines) are all shown.

would also melt part of the planet crust and/or mantle, for which there is little evidence in the geologic record, and such massive impactors are highly unlikely by the time of the Neoproterozoic (Section 4). A simple analytical calculation tends to show that the energy required to deglaciate could only be delivered by an impactor that is larger than 100 km (Text S1 in Supporting Information S1).

The equilibrium spatial temperature profiles (i.e., spatially resolved profiles for the last times shown in Figures 1a–1h) can provide further insight into the climate forcing effects of our stochastic events (Figure 2). Without any stochastic forcing, we observe the usual latitudinal distribution of surface temperatures, with a maximum of ~205 K at the equator and a minimum of ~190 K at the poles.

For a Toba-like eruption, we find that deposition of the volcanic ash leads to greatest temperature rises near the deposition site itself (Figure 2a). Ash deposition affects the surface albedo on a limited area, locally increasing the absorbed flux. For this reason, considering the eruption at 40°N (Figure 2a, red line) centers the peak of the temperature profile to this location, and lower the maximum temperature of about 5 K due to a weaker incoming flux at this latitude. Additionally, for both cases, heat diffusion (atmospheric circulation) allows a global increase of temperature. By accounting for the radiative effect of the clouds and by assuming 800 ppm of CO<sub>2</sub>, the extra warming is around 10 K, independent of latitude and of the eruption location. We note that the results shown here do not account for the ash injected into the stratosphere, which reduces the bond albedo of the planet and thus

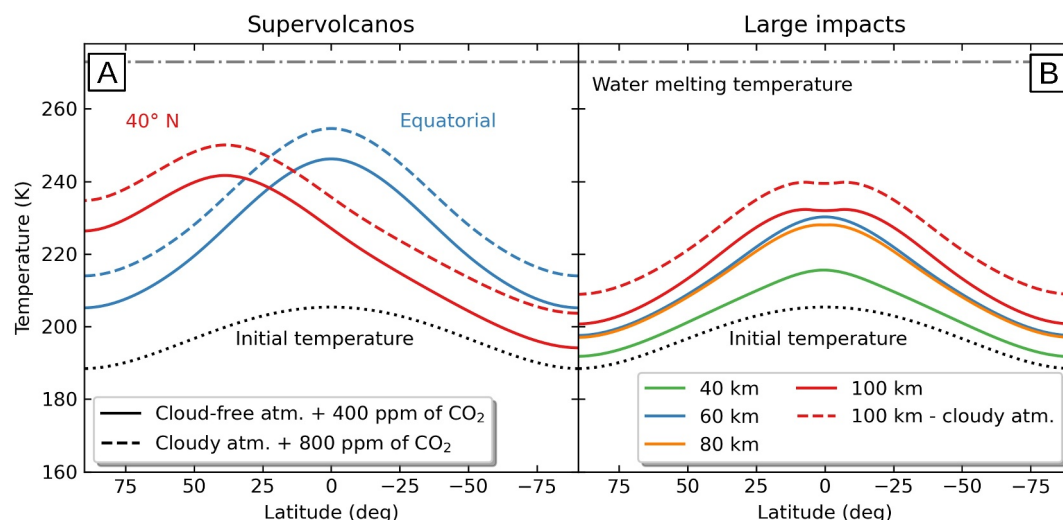


**Figure 2.** Latitudinal temperature profiles after (a) Toba-like eruptions, both at the equator (blue lines) and at 40°N (red lines), and with both the cloud-free atmosphere with 400 ppm CO<sub>2</sub> (solid lines) and an atmosphere including cloud radiative effects and 800 ppm CO<sub>2</sub>, and (b) impacts with impact diameters of 40 km (green), 60 km (blue), 80 km (orange), and 100 km (red), all striking at the equator and under cloud-free atmosphere with 400 ppm CO<sub>2</sub> (solid lines). The red dashed line in panel (b) corresponds to a 100 km impactor under a cloudy atmosphere, assuming 400 ppm of CO<sub>2</sub>. The initial temperature profile (i.e., before climate forcing stochastic events) is shown for both types of events (dotted lines).

induces global cooling (e.g., Abbot & Pierrehumbert, 2010). We discuss such processes, as well as others that we have chosen to neglect in the presented results, and their effect on our conclusions in Section 4.

For impact events, the converged temperature profiles are warmer than the non-perturbed simulation (Figure 2b), due to ejecta affecting the surface albedo. The rise in temperature is a function of the area covered by ejecta: the greater the area covered, the more the albedo of the surface is affected. However, the maximum temperatures for all impact scenarios are colder than those found in scenarios forced by the supervolcanic eruptions. The injection of heat that is provided by the impactors is a relatively minor effect in comparison to the change in surface albedo of the ice that is brought about by the ejecta curtain. Evidence for this can also be found in the temporal evolution of temperatures after the impacts (Figures 1e–1h). In the four cases, the large radiative imbalance at the impact site dissipates heat rapidly relative to the timescale of global temperature changes. Therefore, the colder converged temperatures of our impacts are due to the diminished ejecta coverage that they produce in comparison to the coverage of the supervolcanic ash (see Figure S3 in Supporting Information S1). Interestingly, for 80 and 100 km impactors, we find a cold patch in the converged temperature profile at the impact site. We determine this to be due to the transient water belt that forms after the impact: when the planet cools, this liquid water freezes at the impact site as clean ice with greater albedo than the ejecta-covered ice around the crater.

## 4. Discussion

### 4.1. Limitations of the Climate Model

H<sub>2</sub>O and CO<sub>2</sub> are efficient greenhouse gases and should facilitate the warming and deglaciation of the ice sheet. However, we find that variation of the gas partial pressures, within sensible bounds for the climate of a Neoproterozoic Snowball Earth, cannot push our stochastic events into regimes where they cause global deglaciation (see Text S5 in Supporting Information S1).

There are a variety of effects that are not included in the EBM that could be considered as important. We neglect the formation of stratospheric aerosols, which would act to cool the planet (Macdonald & Wordsworth, 2017). In order to minimize the degrees of freedom in the model, we do not account for ice thickness or the latent heat released by ice melting, which could be important in accounting for the time-scales over which the water belt induced by the 100-km impactor freezes. In much the same way, oceanic circulation will affect the creation of ice in the water belt (e.g., Brunetti et al., 2019; Yang et al., 2020). However, a commonality between these effects is that their inclusion would serve only to increase the challenge in producing global deglaciation, which our models

already suggest is not achievable given the scales of events considered. We thus suggest that our simplified EBM is able to point out possible directions for further works using more complex models.

#### 4.2. Assumptions on Impacts and Large Eruptions

Our simulations suggest that impacts larger than 100 km are necessary, albeit not sufficient, to initiate deglaciation on the planet. However, dynamical models indicate that, outside of the early Solar System, such impacts are expected to occur less than once every billion years (Koeberl & Ivanov, 2019). Moreover, geologic evidence for such event should be present, since a large projectile should have globally spread an ejecta layer analogous to the Chicxulub impact event (Alvarez et al., 1980). So far, no impact signature caused by a  $\sim 100$ -km impactor has been found on Earth (Gyollai et al., 2014; Peucker-Ehrenbrink et al., 2016); as per Allen et al. (2022), the largest impact crater found is caused by a 20–25 km impactor.

The results we present are based on a single impact scenario, comprising of a fixed stratigraphy and an asteroidal projectile hitting the surface at  $17 \text{ km s}^{-1}$ . We chose an ice thickness of 5 km following Erickson et al. (2020) as a reasonable upper limit for the actual size of glaciers covering the planet. In reality, the ice thickness will depend on the location, as suggested by the geologic record (e.g., McMechan, 2000) and climate modeling (Hyde et al., 2000), ranging from meters to 5 km. Variation in ice thickness will produce a mechanically different response to impact. However, given the scale of impactor that our models find would be necessary to cause global deglaciation (i.e.,  $d > 100 \text{ km}$ ), the ice thickness is relatively shallow in comparison, and we thus expect that the consequences of this effect would be minor. Further, we did not consider impactors of alternative compositions, such as icy bodies, in our models. While short-period comets (impact velocity of  $30 \text{ km s}^{-1}$ , Chyba, 1991) have kinetic energies similar to that of the asteroidal impacts we consider, long-period comets ( $50 \text{ km s}^{-1}$ , Chyba, 1991) might change the impact mechanics, but are less likely to hit the Earth (Weissman, 2006). Such events would leave behind a distinct geochemical signal from a rocky impactor analog that, while not yet discovered, should similarly perhaps not be excluded for now. Further modeling of such stochastic events could be entertained by future works, although will likely find challenges of scale similar to our work (i.e., requiring extremely unlikely comet sizes to cause deglaciation). Finally, we assumed zero porosity as a worst case scenario: for a given size, non-porous material ensures the maximum kinetic energy available to melt ice and vapourize target rocks. Similar to the climate choices made, therefore, relaxing this assumption only serves to make deglaciation more challenging.

In modeling volcanic eruptions, results are sensitive to the assumed dust distribution and the absence of lava warming and water vapor. Based on Icelandic dust and ash (Dragosics et al., 2016), a thickness of 15 mm is considered as the threshold for ice to melt due to the decrease in albedo. A thicker layer would thermally insulate the ice below, preventing melting. Increasing such a threshold would expand the dust-covered area subject to melting, favoring deglaciation. Furthermore, the local temperature increase due to erupting lava is disregarded, since its effect is negligible when averaged longitudinally. Similarly, we do not consider a long-term (i.e., multi-year) eruption, which would force a higher temperature around the volcano for a longer time. Additionally, as seen for the Hunga Tonga-Hunga Ha'apai eruption, a substantial amount (up to  $10^{11} \text{ kg}$ ) of water vapor can be injected into the stratosphere where it can have multi-year long radiative effects (net warming of the surface, Millán et al., 2022). Finally, aerosols ejected up to the stratosphere could increase snowfall, thus covering low albedo dusty ice.

#### 4.3. Possible Shortening of Snowball Events

In this work, we consider a low  $\text{CO}_2$  pressure as the initial climate state. However, during a snowball event the carbon cycle is altered due to the ice shield preventing  $\text{CO}_2$  (partial) dissolution into the ocean and restricted silicate weathering on land. On modern Earth,  $\text{CO}_2$  outgassing is about 47 bar/Gyr (Catling & Kasting, 2017) through a combination of continental and submarine volcanism. Although there is no consensus so far on the exact volcanic outgassing flux for snowball Earth, multiple studies suggest that the value was much lower than present day. Fischer and Aiuppa (2020) estimate the arc production around 5.7 bar/Gyr while Dutkiewicz et al. (2024) argue that the mid-ocean ridge outgassing was even lower. We found that an extra radiative forcing of  $50 \text{ W/m}^2$  (in addition to  $14 \text{ W/m}^2$  of forcing induced by the clouds) is required, coupled with the effect of a 100 km impactor, to deglaciate the planet. That is corresponding approximately to 0.08 bar of  $\text{CO}_2$  according to Wolf et al. (2018). In comparison, without any stochastic event the required forcing to deglaciate is equal to  $90 \text{ W/m}^2$

(in addition to  $14 \text{ W/m}^2$  of forcing induced by the clouds). Using modern day Earth outgassing from Fischer and Aiuppa (2020) as boundary values, it takes between 1.7 and 14 Myr to reach a  $\text{CO}_2$  pressure for which a 100-km impactor could induce a deglaciation, in our framework. An intermediate outgassing value of 25 bar/Gyr gives approximately 3.2 Myr to reach the required  $\text{CO}_2$  pressure.

These estimates should be considered as lower limits because we neglect the potential sinks of  $\text{CO}_2$  existing on snowball Earth, as well as cooling processes of impacts (e.g., increase of the bond albedo due to aerosols). However, this timescale is shorter than the duration time of the Marinoan and Sturtian glaciations. Although a large impact during this period seems highly unlikely, the possibility of deglaciating an extra-solar planet in this way cannot be ruled out.

## 5. Conclusions

Earth's periods of global glaciation are traditionally conceived to have ended through a gradual build-up greenhouse gases in the atmosphere (e.g.,  $\text{CO}_2$ ). However, the shortest of these so-called Snowball Earth states were geologically short and stochastic events such as impacts and supervolcanic eruptions has been suggested as plausible deglaciation processes. Here, we present modeling on the response of Snowball Earth to such events under differing scenarios. We use impact simulations and ash spreading models to estimate the initial effect of each stochastic event, and follow these up by evolving Earth's surface environment through time using a 1-D EBM.

In our modeling framework, surface albedo of the planet is the dominant driving force of long-term temperature change in the aftermath of stochastic events. For impacts, this takes the form of the ejecta curtain stemming from the impact site. For eruptions, volcanic ash is transported over a wide range of latitude and longitudes. We thus observe that eruptions produce a greater change in Earth's surface albedo and hence a greater temperature response for typical scale events. However, even an impactor radius of 100 km is not sufficient to induce deglaciation of Snowball Earth. The warming at the impact site melts ice locally in the short-term, but due to a large radiative local imbalance, ice reforms in less than a year, returning the planet to the snowball state. Even if larger impactors could induce deglaciation, they are dynamically unlikely to have occurred on Earth at the time of its snowball episodes. Similarly, no recorded supervolcanic eruption could have single-handedly deglaciated Earth. The surface temperature increase due to dust deposition from the largest recorded event, Toba, does not reach the melting temperature of ice anywhere on the planet.

Our model thus places constraints on the magnitude of stochastic events that are incapable of triggering Snowball Earth termination. However, these constraints should be refined with more comprehensive modeling. For impacts, 3-D modeling can better resolve the ejecta distribution through accounting for oblique impacts. Impact simulations should also be able to account for the ice erosion effect due to the tsunami created upon impact, which would increase the low-albedo area. For the climate response, 3-D Global Climate Model (GCM) modeling is required to include longitudinal and vertical resolutions, as well as to provide better representations of clouds, rain/snow, atmospheric dynamics, ocean dynamics, and distribution of aerosols ejected by the impactor (e.g., Abbot et al., 2011; Ashkenazy et al., 2013; Turbet et al., 2020) or released by the volcano (McGraw et al., 2024). For instance, even 2-D models could show more complex transitions between two steady states if specific eigenmodes are triggered by an impact happening at the right location (Bastiaansen et al., 2022; Mulder et al., 2021).

Lastly, in this work, we treated impacts and supervolcanoes as independent and instantaneous events all starting from the same initial state. Future analyses should investigate some of the prolonged effects associated with our stochastic events (e.g., multi-year lava eruptions). Additionally, the combined effect of impacts and eruptions should be considered, with impact-induced volcanism having been suggested as a potential supplement for the K-T extinction (e.g., Renne et al., 2015), although still debated (e.g., Bhandari et al., 1995). Multiple such events would likely stack their temperature responses, although unlikely to be in a linear manner, and could thus instigate a deglaciation of Snowball Earth.

## Conflict of Interest

The authors declare no conflicts of interest relevant to this study.

## Data Availability Statement

At present, the iSALE code (Collins et al., 2016) is not fully open-source. It is distributed via a private GitHub repository on a case-by-case basis to academic users in the impact community, strictly for non-commercial use. The temperature profile after impact, used to perform climate simulations can be found from Chaverot et al. (2024).

## Acknowledgments

The project was made possible by the 2022 Cooperative Institute for Dynamic Earth Research (CIDER) workshop in UC Berkeley, funded by the NSF. This work has been carried out within the framework of the NCCR PlanetS supported by the Swiss National Science Foundation under Grants 51NF40\_182901 and 51NF40\_205606. GC acknowledges the financial support of the SNSF (Grant 200021\_197176, 200020\_215760, and P500PT\_217840). AZ acknowledges the financial support of Stanford University. II was supported by the UK Science and Technology Facilities Council (STFC) Grant ST/T505985/1. RG acknowledges funding by the National Aeronautics and Space Administration (NASA) through a contract with ORAU. We gratefully acknowledge the developers of iSALE-2D, including Gareth Collins, Kai Wünnemann, Dirk Elbeshausen, Tom Davison, Boris Ivanov and Jay Melosh. Authors gratefully acknowledge R. T. Pierrehumbert for useful discussions during the 2022 CIDER workshop. We thank the two anonymous reviewers for the time they spent providing useful comments that helped to improve this manuscript.

## References

- Abbot, D. S. (2014). Resolved Snowball Earth clouds. *Journal of Climate*, 27(12), 4391–4402. <https://doi.org/10.1175/JCLI-D-13-00738.1>
- Abbot, D. S., & Pierrehumbert, R. T. (2010). Mudball: Surface dust and Snowball Earth deglaciation. *Journal of Geophysical Research*, 115(D3), D03104. <https://doi.org/10.1029/2009JD012007>
- Abbot, D. S., Voigt, A., & Koll, D. (2011). The Jormungand global climate state and implications for Neoproterozoic glaciations. *Journal of Geophysical Research*, 116(D18), D18103. <https://doi.org/10.1029/2011JD015927>
- Allen, N. H., Nakajima, M., Wünnemann, K., Helhoski, S., & Trail, D. (2022). A revision of the formation conditions of the Vredefort crater. *Journal of Geophysical Research: Planets*, 127(8), e2022JE007186. <https://doi.org/10.1029/2022JE007186>
- Alvarez, L. W., Alvarez, W., Asaro, F., & Michel, H. V. (1980). Extraterrestrial cause for the cretaceous-tertiary extinction. *Science*, 208(4448), 1095–1108. <https://doi.org/10.1126/science.208.4448.1095>
- Artemieva, N., Morgan, J., & Party, E. S. (2017). Quantifying the release of climate-active gases by large meteorite impacts with a case study of Chicxulub. *Geophysical Research Letters*, 44(20), 10180–10188. <https://doi.org/10.1002/2017GL074879>
- Ashkenazy, Y., Gildor, H., Losch, M., Macdonald, F. A., Schrag, D. P., & Tziperman, E. (2013). Dynamics of a Snowball Earth ocean. *Nature*, 495(7439), 90–93. <https://doi.org/10.1038/nature11894>
- Bastiaansen, R., Dijkstra, H. A., & Heydt, A. S. V. D. (2022). Fragmented tipping in a spatially heterogeneous world. *Environmental Research Letters*, 17(4), 045006. <https://doi.org/10.1088/1748-9326/ac59a8>
- Batchelor, C. L., Margold, M., Krapp, M., Murton, D. K., Dalton, A. S., Gibbard, P. L., et al. (2019). The configuration of northern hemisphere ice sheets through the quaternary. *Nature Communications*, 10(1), 3713. <https://doi.org/10.1038/s41467-019-11601-2>
- Benz, W., Cameron, A. G. W., & Melosh, H. J. (1989). The origin of the Moon and the single-impact hypothesis III. *Icarus*, 81(1), 113–131. [https://doi.org/10.1016/0019-1035\(89\)90129-2](https://doi.org/10.1016/0019-1035(89)90129-2)
- Bhandari, N., Shukla, P. N., Ghevariya, Z. G., & Sundaram, S. M. (1995). Impact did not trigger Deccan volcanism: Evidence from Anjar K/T boundary intertrappean sediments. *Geophysical Research Letters*, 22(4), 433–436. <https://doi.org/10.1029/94GL03271>
- Brugger, J., Feulner, G., & Petri, S. (2017). Baby, it's cold outside: Climate model simulations of the effects of the asteroid impact at the end of the Cretaceous. *Geophysical Research Letters*, 44(1), 419–427. <https://doi.org/10.1002/2016GL072241>
- Brunetti, M., Kasparian, J., & V erard, C. (2019). Co-existing climate attractors in a coupled aquaplanet. *Climate Dynamics*, 53(9), 6293–6308. <https://doi.org/10.1007/s00382-019-04926-7>
- Budyko, M. I. (1969). The effect of solar radiation variations on the climate of the Earth. *Tellus*, 21(5), 611–619. <https://doi.org/10.1111/j.2153-3490.1969.tb00466.x>
- Caldeira, K., & Kasting, J. F. (1992). Susceptibility of the early Earth to irreversible glaciation caused by carbon dioxide clouds. *Nature*, 359(6392), 226–228. <https://doi.org/10.1038/359226a0>
- Catling, D. C., & Kasting, J. F. (2017). Atmospheric evolution on inhabited and lifeless worlds.
- Chaverot, G., Zorzi, A., Ding, X., Itcovitz, J., Fan, B., Bhatnagar, S., et al. (2024). Resilience of Snowball Earth to stochastic events [Dataset]. *Zenodo*. <https://doi.org/10.5281/zenodo.10286185>
- Chumakov, N. (2009). The Baykonurian glaciohorizon of the late Vendian. *Stratigraphy and Geological Correlation*, 17(4), 373–381. <https://doi.org/10.1134/S0869593809040029>
- Chyba, C. F. (1991). Terrestrial mantle siderophiles and the lunar impact record. *Icarus*, 92(2), 217–233. [https://doi.org/10.1016/0019-1035\(91\)90047-W](https://doi.org/10.1016/0019-1035(91)90047-W)
- Cisneros de Le on, A., Mittal, T., de Silva, S. L., Self, S., Schmitt, A. K., & Kutterolf, S. (2022). On synchronous supereruptions. *Frontiers in Earth Science*, 10, 827252. <https://doi.org/10.3389/feart.2022.827252>
- Collins, G. S., Elbeshausen, D., Davison, T. M., Wünnemann, K., Ivanov, B., & Melosh, H. J. (2016). iSALE-Dellen manual. <https://doi.org/10.6084/m9.figshare.3473690.v2>
- Costa, A., Smith, V. C., Macedonio, G., & Matthews, N. E. (2014). The magnitude and impact of the Youngest Toba Tuff super-eruption. *Frontiers in Earth Science*, 2, 16. <https://doi.org/10.3389/feart.2014.00016>
- de Silva, S., & Self, S. (2022). Capturing the extreme in volcanology: The case for the term “Supervolcano”. *Frontiers in Earth Science*, 10, 859237. <https://doi.org/10.3389/feart.2022.859237>
- Dragosics, M., Meinander, O., J onsd ottir, T., D urig, T., De Leeuw, G., P alsson, F., et al. (2016). Insulation effects of Icelandic dust and volcanic ash on snow and ice. *Arabian Journal of Geosciences*, 9(2), 126. <https://doi.org/10.1007/s12517-015-2224-6>
- Dressing, C. D., Spiegel, D. S., Scharf, C. A., Menou, K., & Raymond, S. N. (2010). Habitable climates: The influence of eccentricity. *The Astrophysical Journal*, 721(2), 1295–1307. <https://doi.org/10.1088/0004-637X/721/2/1295>
- Dutkiewicz, A., Merdith, A. S., Collins, A. S., Mather, B., Ilano, L., Zahirovic, S., & M uller, R. D. (2024). Duration of Sturtian “Snowball Earth” glaciation linked to exceptionally low mid-ocean ridge outgassing. *Geology*, 52(4), 292–296. <https://doi.org/10.1130/G51669.1>
- Erickson, T. M., Kirkland, C. L., Timms, N. E., Cavosie, A. J., & Davison, T. M. (2020). Precise radiometric age establishes Yarrabubba, Western Australia, as Earth’s oldest recognised meteorite impact structure. *Nature Communications*, 11(1), 300. <https://doi.org/10.1038/s41467-019-13985-7>
- Fischer, T. P., & Aiuppa, A. (2020). AGU centennial grand challenge: Volcanoes and deep carbon global CO<sub>2</sub> emissions from subaerial volcanism —Recent progress and future challenges. *Geochemistry, Geophysics, Geosystems*, 21(3), e2019GC008690. <https://doi.org/10.1029/2019GC008690>
- Flanner, M. G., Arnheim, J. B., Cook, J. M., Dang, C., He, C., Huang, X., et al. (2021). SNICAR-ADv3: A community tool for modeling spectral snow albedo. *Geoscientific Model Development*, 14(12), 7673–7704. <https://doi.org/10.5194/gmd-14-7673-2021>
- Ghil, M. (1994). Cryothermodynamics: The chaotic dynamics of paleoclimate. *Physica D: Nonlinear Phenomena*, 77(1–3), 130–159. [https://doi.org/10.1016/0167-2789\(94\)90131-7](https://doi.org/10.1016/0167-2789(94)90131-7)

- Gyollai, I., Mader, D., Polgári, M. P., Popp, F., & Koeberl, C. (2014). Lack of evidence for impact signatures in Neoproterozoic postglacial deposits from NW-Namibia. *Austrian Journal of Earth Sciences*, 102(2), 100–111.
- Hambrey, M. J., & Harland, W. B. (1981). *Earth's pre-Pleistocene glacial record*. Cambridge University Press.
- Hansen, J. E., Wang, W.-C., & Lacis, A. A. (1978). Mount Agung eruption provides test of a global climatic perturbation. *Science*, 199(4333), 1065–1068. <https://doi.org/10.1126/science.199.4333.1065>
- Harland, W. B. (1964). Critical evidence for a great infra-Cambrian glaciation. *Geologische Rundschau*, 54(1), 45–61. <https://doi.org/10.1007/BF01821169>
- Hoffman, P. F., Abbot, D. S., Ashkenazy, Y., Benn, D. I., Brooks, J. J., Cohen, P. A., et al. (2017). Snowball Earth climate dynamics and Cryogenian geology-geobiology. *Science Advances*, 3(11), e1600983. <https://doi.org/10.1126/sciadv.1600983>
- Hoffman, P. F., Kaufman, A. J., Halverson, G. P., & Schrag, D. P. (1998). A neoproterozoic Snowball Earth. *Science*, 281(5381), 1342–1346. <https://doi.org/10.1126/science.281.5381.1342>
- Hotelling, S., Lutz, S., Dial, R. J., Anesio, A. M., Benning, L. G., Fountain, A. G., et al. (2021). Biological albedo reduction on ice sheets, glaciers, and snowfields. *Earth-Science Reviews*, 220, 103728. <https://doi.org/10.1016/j.earscirev.2021.103728>
- Hyde, W. T., Crowley, T. J., Baum, S. K., & Peltier, W. R. (2000). Neoproterozoic 'Snowball Earth' simulations with a coupled climate/ice-sheet model. *Nature*, 405(6785), 425–429. <https://doi.org/10.1038/35013005>
- Kennedy, M. J. (1996). Stratigraphy, sedimentology, and isotopic geochemistry of Australian Neoproterozoic postglacial cap dolostones; deglaciation, delta 13 C excursions, and carbonate precipitation. *Journal of Sedimentary Research*, 66(6), 1050–1064. <https://doi.org/10.2110/jsr.66.1050>
- Kirschvink, J. L. (1992). Late Proterozoic low-latitude global glaciation: The Snowball Earth. In J. Schopf & C. Klein (Eds.), *In the Proterozoic biosphere: A multidisciplinary study*. Cambridge University Press. <https://doi.org/10.1017/CBO9780511601064>
- Knoll, A., Hayes, J., Kaufman, A., Swett, K., & Lambert, I. (1986). Secular variation in carbon isotope ratios from upper Proterozoic successions of Svalbard and east Greenland. *Nature*, 321(6073), 832–838. <https://doi.org/10.1038/321832a0>
- Koeberl, C., & Ivanov, B. A. (2019). Asteroid impact effects on Snowball Earth. *Meteoritics & Planetary Sciences*, 54(10), 2273–2285. <https://doi.org/10.1111/maps.13294>
- Kring, D. A. (2003). Environmental consequences of impact cratering events as a function of ambient conditions on Earth. *Astrobiology*, 3(1), 133–152. <https://doi.org/10.1089/153110703321632471>
- Lan, Z., Huyskens, M. H., Le Hir, G., Mitchell, R. N., Yin, Q.-Z., Zhang, G., & Li, X.-H. (2022). Massive volcanism may have foreshortened the Marinoan Snowball Earth. *Geophysical Research Letters*, 49(6), e2021GL097156. <https://doi.org/10.1029/2021GL097156>
- Le Feuvre, M., & Wieczorek, M. A. (2011). Nonuniform cratering of the moon and a revised crater chronology of the inner solar system. *Icarus*, 214(1), 1–20. <https://doi.org/10.1016/j.icarus.2011.03.010>
- Le Hir, G., Donnadieu, Y., Krinner, G., & Ramstein, G. (2010). Toward the Snowball Earth deglaciation. *Climate Dynamics*, 35(2–3), 285–297. <https://doi.org/10.1007/s00382-010-0748-8>
- Macdonald, F. A., & Wordsworth, R. (2017). Initiation of Snowball Earth with volcanic sulfur aerosol emissions. *Geophysical Research Letters*, 44(4), 1938–1946. <https://doi.org/10.1002/2016GL072335>
- Mason, B. G., Pyle, D. M., & Oppenheimer, C. (2004). The size and frequency of the largest explosive eruptions on Earth. *Bulletin of Volcanology*, 66(8), 735–748. <https://doi.org/10.1007/s00445-004-0355-9>
- McGraw, Z., DallaSanta, K., Polvani, L. M., Tsigaridis, K., Orbe, C., & Bauer, S. E. (2024). Severe global cooling after volcanic super-eruptions? The answer hinges on unknown aerosol size. *Journal of Climate*, 37(4), 1449–1464. <https://doi.org/10.1175/JCLI-D-23-0116.1>
- McMechan, M. (2000). Vreeland diamictites – Neoproterozoic glaciogenic slope deposits, Rocky Mountains, northeast British Columbia. *Bulletin of Canadian Petroleum Geology*, 48(3), 246–261. <https://doi.org/10.2113/48.3.246>
- Menou, K. (2015). Climate stability of habitable Earth-like planets. *Earth and Planetary Science Letters*, 429, 20–24. <https://doi.org/10.1016/j.epsl.2015.07.046>
- Millán, L., Santee, M. L., Lambert, A., Livesey, N. J., Werner, F., Schwartz, M. J., et al. (2022). The Hunga Tonga–Hunga Ha'apai hydration of the stratosphere. *Geophysical Research Letters*, 49(13), e2022GL099381. <https://doi.org/10.1029/2022GL099381>
- Mulder, T. E., Goelzer, H., Wubs, F. W., & Dijkstra, H. A. (2021). Snowball Earth bifurcations in a fully-implicit Earth system model. *International Journal of Bifurcation and Chaos*, 31(06), 2130017. <https://doi.org/10.1142/S0218127421300172>
- North, G. R., & Coakley, J. A., Jr. (1979). Differences between seasonal and mean annual energy balance model calculations of climate and climate sensitivity. *Journal of the Atmospheric Sciences*, 36(7), 1189–1204. [https://doi.org/10.1175/1520-0469\(1979\)036<1189:DBSAMA>2.0.CO;2](https://doi.org/10.1175/1520-0469(1979)036<1189:DBSAMA>2.0.CO;2)
- Peucker-Ehrenbrink, B., Waters, C. A., Kurz, M. D., & Hoffman, P. F. (2016). No evidence of extraterrestrial noble metal and helium anomalies at Marinoan glacial termination. *Earth and Planetary Science Letters*, 437, 76–88. <https://doi.org/10.1016/j.epsl.2015.12.040>
- Pierazzo, E., Kring, D. A., & Melosh, H. J. (1998). Hydrocode simulation of the Chicxulub impact event and the production of climatically active gases. *Journal of Geophysical Research*, 103(E12), 28607–28625. <https://doi.org/10.1029/98JE02496>
- Pyle, D. M. (1989). The thickness, volume and grainsize of tephra fall deposits. *Bulletin of Volcanology*, 51, 1–15. <https://doi.org/10.1007/BF01086757>
- QGIS Development Team. (2024). QGIS geographic information system [Computer software manual]. Retrieved from <https://www.qgis.org>
- Renne, P. R., Sprain, C. J., Richards, M. A., Self, S., Vanderkluyzen, L., & Pande, K. (2015). State shift in Deccan volcanism at the Cretaceous–Paleogene boundary, possibly induced by impact. *Science*, 350(6256), 76–78. <https://doi.org/10.1126/science.aac7549>
- Richardson, J. E., Melosh, H. J., Greenberg, R. J., & O'Brien, D. P. (2005). The global effects of impact-induced seismic activity on fractured asteroid surface morphology. *Icarus*, 179(2), 325–349. <https://doi.org/10.1016/j.icarus.2005.07.005>
- Rooney, A. D., Strauss, J. V., Brandon, A. D., & Macdonald, F. A. (2015). A Cryogenian chronology: Two long-lasting synchronous Neoproterozoic glaciations. *Geology*, 43(5), 459–462. <https://doi.org/10.1130/G36511.1>
- Rose, W. I., & Chesner, C. A. (1990). Worldwide dispersal of ash and gases from Earth's largest known eruption: Toba, Sumatra, 75 ka. *Palaeogeography, Palaeoclimatology, Palaeoecology*, 89(3), 269–275. [https://doi.org/10.1016/0921-8181\(90\)90023-6](https://doi.org/10.1016/0921-8181(90)90023-6)
- Sellers, W. D. (1969). A global climatic model based on the energy balance of the Earth-atmosphere system. *Journal of Applied Meteorology and Climatology*, 8(3), 392–400. [https://doi.org/10.1175/1520-0450\(1969\)008<0392:AGCMBO>2.0.CO;2](https://doi.org/10.1175/1520-0450(1969)008<0392:AGCMBO>2.0.CO;2)
- Shields, A. L., Bitz, C. M., Meadows, V. S., Joshi, M. M., & Robinson, T. D. (2014). Spectrum-driven planetary deglaciation due to increases in stellar luminosity. *The Astrophysical Journal*, 785(1), L9. <https://doi.org/10.1088/2041-8205/785/1/L9>
- Spiegel, D. S., Menou, K., & Scharf, C. A. (2008). Habitable climates. *The Astrophysical Journal*, 681(2), 1609–1623. <https://doi.org/10.1086/588089>
- Turbet, M., Bolmont, E., Chaverot, G., Ehrenreich, D., Leconte, J., & Marq, E. (2021). Day–night cloud asymmetry prevents early oceans on Venus but not on Earth. *Nature*, 598(7880), 276–280. <https://doi.org/10.1038/s41586-021-03873-w>

- Turbet, M., Gillmann, C., Forget, F., Baudin, B., Palumbo, A., Head, J., & Karatekin, O. (2020). The environmental effects of very large bolide impacts on early Mars explored with a hierarchy of numerical models. *Icarus*, 335, 113419. <https://doi.org/10.1016/j.icarus.2019.113419>
- Walker, J. C., Hays, P., & Kasting, J. F. (1981). A negative feedback mechanism for the long-term stabilization of Earth's surface temperature. *Journal of Geophysical Research*, 86(C10), 9776–9782. <https://doi.org/10.1029/jc086ic10p09776>
- Warren, S. G. (1982). Optical properties of snow. *Reviews of Geophysics*, 20(1), 67–89. <https://doi.org/10.1098/rsta.2018.0161>
- Warren, S. G., Brandt, R. E., Grenfell, T. C., & McKay, C. P. (2002). Snowball Earth: Ice thickness on the tropical ocean. *Journal of Geophysical Research*, 107(C10), 31-1–31-18. <https://doi.org/10.1029/2001JC001123>
- Weissman, P. R. (2006). The cometary impactor flux at the Earth. *Proceedings of the International Astronomical Union*, 2(S236), 441–450. <https://doi.org/10.1017/S1743921307003559>
- Williams, D. M., & Kasting, J. F. (1997). Habitable planets with high obliquities. *Icarus*, 129(1), 254–267. <https://doi.org/10.1006/icar.1997.5759>
- Williams, D. M., Kasting, J. F., & Frakes, L. A. (1998). Low-latitude glaciation and rapid changes in the Earth's obliquity explained by obliquity–oblateness feedback. *Nature*, 396(6710), 453–455. <https://doi.org/10.1038/24845>
- Wolf, E. T., Haqq-Misra, J., & Toon, O. B. (2018). Evaluating climate sensitivity to CO<sub>2</sub> across Earth's history. *Journal of Geophysical Research: Atmospheres*, 123(21), 11861–11874. <https://doi.org/10.1029/2018JD029262>
- Yang, J., Ji, W., & Zeng, Y. (2020). Transition from eyeball to snowball driven by sea-ice drift on tidally locked terrestrial planets. *Nature Astronomy*, 4(1), 58–66. <https://doi.org/10.1038/s41550-019-0883-z>

## References From the Supporting Information

- Amsden, A. A., Ruppel, H. M., & Hirt, C. W. (1980). *SALE: A simplified ALE computer program for fluid flow at all speeds* (Tech. Rep.). Los Alamos Scientific Laboratories. <https://doi.org/10.2172/5176006>
- Berger, A. (1978). Long-term variations of daily insolation and quaternary climatic changes. *Journal of the Atmospheric Sciences*, 35(12), 2362–2367. [https://doi.org/10.1175/1520-0469\(1978\)035<2362:LTVOVDI>2.0.CO;2](https://doi.org/10.1175/1520-0469(1978)035<2362:LTVOVDI>2.0.CO;2)
- Chaverot, G., Turbet, M., Bolmont, E., & Leconte, J. (2022). How does the background atmosphere affect the onset of the runaway greenhouse? *Astronomy & Astrophysics*, 658, A40. <https://doi.org/10.1051/0004-6361/202142286>
- Collins, G. S. (2014). Numerical simulations of impact crater formation with dilatancy. *Journal of Geophysical Research: Planets*, 119(12), 2600–2619. <https://doi.org/10.1002/2014JE004708>
- Collins, G. S., Melosh, H. J., & Ivanov, B. A. (2004). Modeling damage and deformation in impact simulations. *Meteoritics & Planetary Sciences*, 39(2), 217–231. <https://doi.org/10.1111/j.1945-5100.2004.tb00337.x>
- Collins, G. S., Melosh, H. J., & Wünnemann, K. (2011). Improvements to the  $\epsilon - \alpha$  porous compaction model for simulating impacts into high-porosity solar system objects. *International Journal of Impact Engineering*, 38(6), 434–439. <https://doi.org/10.1016/j.ijimpeng.2010.10.013>
- Collins, G. S., Patel, N., Davison, T. M., Rae, A. S. P., Morgan, J. V., Gulick, S. P. S., et al. (2020). A steeply-inclined trajectory for the Chicxulub impact. *Nature Communications*, 11(1), 1480. <https://doi.org/10.1038/s41467-020-15269-x>
- Ivanov, B. A., Deniem, D., & Neukum, G. (1997). Implementation of dynamic strength models into 2D hydrocodes: Applications for atmospheric breakup and impact cratering. *International Journal of Impact Engineering*, 20(1), 411–430. [https://doi.org/10.1016/S0734-743X\(97\)87511-2](https://doi.org/10.1016/S0734-743X(97)87511-2)
- Kasting, J. F. (1988). Runaway and moist greenhouse atmospheres and the evolution of Earth and Venus. *Icarus*, 74(3), 472–494. [https://doi.org/10.1016/0019-1035\(88\)90116-9](https://doi.org/10.1016/0019-1035(88)90116-9)
- Koll, D. D., & Cronin, T. W. (2018). Earth's outgoing longwave radiation linear due to H<sub>2</sub>O greenhouse effect. *Proceedings of the National Academy of Sciences*, 115(41), 10293–10298. <https://doi.org/10.1073/pnas.1809868115>
- Kring, D. A. (2007). The Chicxulub impact event and its environmental consequences at the Cretaceous–Tertiary boundary. *Palaeogeography, Palaeoclimatology, Palaeoecology*, 255(1), 4–21. <https://doi.org/10.1016/j.palaeo.2007.02.037>
- Leconte, J., Forget, F., Charnay, B., Wordsworth, R., & Pottier, A. (2013). Increased insolation threshold for runaway greenhouse processes on Earth like planets. *Nature*, 504(7479), 268–271. <https://doi.org/10.1038/nature12827>
- Melosh, H. J., Ryan, E. V., & Asphaug, E. (1992). Dynamic fragmentation in impacts: Hydrocode simulation of laboratory impacts. *Journal of Geophysical Research*, 97(E9), 14735–14759. <https://doi.org/10.1029/92JE01632>
- Pierrehumbert, R. T., Abbot, D. S., Voigt, A., & Koll, D. (2011). Climate of the Neoproterozoic. *Annual Review of Earth and Planetary Sciences*, 39(1), 417–460. <https://doi.org/10.1146/annurev-earth-040809-152447>
- Thompson, S. L., & Lauson, H. S. (1974). *Improvements in the CHART D radiationhydrodynamic code III: Revised analytic equations of state* (Tech. Rep. No. SC-RR-71-0714). Sandia Laboratories.
- Wagner, T. J., & Eisenman, I. (2015). How climate model complexity influences sea ice stability. *Journal of Climate*, 28(10), 3998–4014. <https://doi.org/10.1175/jcli-d-14-00654.1>
- Wünnemann, K., Collins, G. S., & Melosh, H. J. (2006). A strain-based porosity model for use in hydrocode simulations of impacts and implications for transient crater growth in porous targets. *Icarus*, 180(2), 514–527. <https://doi.org/10.1016/j.icarus.2005.10.013>
- Wünnemann, K., Collins, G. S., & Osinski, G. R. (2008). Numerical modelling of impact melt production in porous rocks. *Earth and Planetary Science Letters*, 269(3), 530–539. <https://doi.org/10.1016/j.epsl.2008.03.007>